

Theoretical Studies of Molecular Structures, Infrared Spectra, NBO and NLO Properties of Some Novel 5-arylazo-6-hydroxy-4-phenyl-3-cyano-2-pyridone Dyes

A. ESME^{a,*} AND S.G. SAGDINC^b

^aDepartment of Elementary Science Education, Kocaeli University, 41380, Umuttepe, Kocaeli, Turkey

^bDepartment of Physics, Science and Art Faculty, Kocaeli University, 41380, Umuttepe, Kocaeli, Turkey

(Received February 18, 2016; in final form November 5, 2016)

The optimized geometrical structures, infrared spectra, molecular electrostatic potential, natural bond orbital and nonlinear optical properties of 5-phenylazo-6-hydroxy-4-phenyl-3-cyano-2-pyridone (1) and 5-(4-bromophenylazo)-6-hydroxy-4-phenyl-3-cyano-2-pyridone (2) dyes with a detailed study on the azo-hydrazone tautomerism in the ground state have been investigated by density functional theory using B3LYP functional with 6-31G(d,p) basis set. Vibrational modes are assigned with the help of vibrational energy distribution analysis program. Highest occupied molecular orbital and lowest unoccupied molecular orbital energies of the (1) and (2) compounds with azo and hydrazone forms were calculated with the same method and basis set. Molecular parameters like global hardness (η), global softness (σ) and electronegativity (χ) were calculated with the results obtained from the highest occupied and lowest unoccupied molecular orbital energies. Nonlinear optical parameters (mean polarizability ($\langle\alpha\rangle$), the anisotropy of the polarizability ($\langle\Delta\alpha\rangle$) and the mean first-order hyperpolarizability ($\langle\beta\rangle$) of the title compounds were investigated theoretically. The atomic charges, electronic exchange interaction, and charge delocalization of the molecules have been studied by natural bond orbital analysis.

DOI: [10.12693/APhysPolA.130.1273](https://doi.org/10.12693/APhysPolA.130.1273)

PACS/topics: 31.15.E-, 33.20.Ea, 31.50.Bc, 42.65.-k

1. Introduction

Azo dyes containing at least a chromophore azo group ($-\text{N}=\text{N}-$) are an important class of synthetic organic colorants which are extensively used in the dyestuffs industry and also, more recently, in the field of non-linear optics [1]. There has been growing interest in the non-linear optical (NLO) properties of azo materials for their large nonlinear refraction which are interesting for the application in optical storage capacity, optical-limiting and optical switching application [2]. Besides, the arylazo colorants belonging to the azo dyes class are a very important class of colorants. The importance of arylazo pyridone dyes containing pyridone rings have increased due to the use of polyester and nylon as the main synthetic fibers. Azo pyridone dyes have largely replaced yellow disperse dyes based on pyrazolones due to their bright hues and suitability for the dyeing of polyester fabrics [3, 4]. Pyridone disperse yellow dyes, such as C.I. Disperse Yellows 114, 119, and 211, are used for dyeing polyester fabrics [5, 6].

Pyridone derivatives are relatively recent heterocyclic intermediates for the preparation of arylazo dyes and several investigations on substituted arylazo pyridone dyes have been carried out and reviewed [7–9]. The physico-chemical properties of arylazo pyridone dyes are closely related to their azo and hydrazone tautomerism which occurs in azo dyes bearing groups with labile proton conjugated with azo linkage. It has been concluded that the

equilibrium between the two tautomers is influenced by the structure of the compounds [10].

In the previous publication, a series of some novel arylazo pyridone dyes have been synthesized (Fig. 1) by Alimmari et al. [11]. The structures of 5-phenylazo-6-hydroxy-4-phenyl-3-cyano-2-pyridone (1) and 5-(4-bromophenylazo)-6-hydroxy-4-phenyl-3-cyano-2-pyridone (2) dyes were experimentally confirmed by UV-vis, the Fourier transform infrared (FT-IR), ¹H-NMR and ¹³C-NMR spectroscopic techniques and elemental analysis. Literature survey reveals that so far there is no complete theoretical calculation on the (1) and (2) molecules published which has motivated us to undertake a detailed quantum mechanical analysis for understanding the structural, electronic and NLO properties, natural bond orbital (NBO) analysis and vibrational studies for the azo and hydrazone forms of some arylazo pyridone dyes, (1) and (2), using (density functional theory, DFT) B3LYP/6-31G(d,p) method. Therefore, the aim of this study is to fully determine the molecular structures, FT-IR spectra and assignments, frontier molecular orbital energies, molecular electrostatic potential and nonlinear optical properties of (1) and (2) dyes. Detailed interpretations of the vibrational spectra of (1) and (2) compounds have been made based on the calculated percentage potential energy distribution (PED).

2. Computational procedure

All calculations of the (1) and (2) molecules have been performed using the Gaussian 09 Rev. A 11.4 [12] software package and the output files were visualized by means of the GaussView Rev. 5.0.9 [13] software.

*corresponding author; e-mail: asli.esme@kocaeli.edu.tr

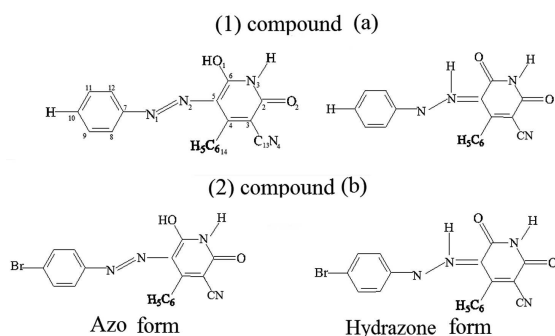


Fig. 1. Azo-hydrazone tautomerism in studied arylazo pyridine dyes.

The full geometrical optimization of the title compounds in the gas phase were carried out using the B3LYP/6-31G(d,p) method. The DFT calculations were performed using Becke's three-parameter hybrid functional [14] with the Lee–Yang–Parr correlation functional [15], a combination that gives rise to the well-known B3LYP method. The optimized structure parameters (bond lengths and dihedral angles), vibrational frequencies, IR and Raman intensities of title compounds were calculated by using B3LYP/6-31G(d,p) method. The theoretical vibrational modes of (1) and (2) compounds using percentage potential energy distribution (PED) have been done with the VEDA4 program written by Jamroz [16]. At the optimized structures of the molecules no imaginary frequency modes were obtained, providing that a true minimum on the potential energy surface was found. The vibrational frequencies obtained from the B3LYP calculations have been scaled by a factor of 0.9608 [17], which is a typical correction factor for B3LYP frequencies [18]. Highest occupied molecular orbital (HOMO) and lowest unoccupied molecular orbital (LUMO) calculations were made at the same level of theory. The natural bond orbital (NBO) calculations were performed using NBO 3.1 program [19] as implemented in the Gaussian 09 [12] package at the B3LYP/6-31G(d,p) level in order to understand various second order interactions between the filled orbitals of one subsystem and vacant orbitals of another subsystem, which is a measure of the intermolecular delocalization or hyper conjugation.

In the context of the HF theorem, the E_{HOMO} and E_{LUMO} is used to approximate the ionization potential (I) and electron affinity (A) given by Koopmans' theorem [20], respectively. Although no formal proof of this theorem exists within DFT, its validity is generally accepted. DFT has shown to be successful in providing insights into the chemical reactivity, in terms of molecular parameters such as global hardness (η), global softness (σ), and electronegativity (χ).

I and A are related to

$$I = -E_{\text{HOMO}}, \quad A = -E_{\text{LUMO}}. \quad (1)$$

The global hardness (η) is a measure of the resistance of an atom to charge transfer [21] and it can be calcu-

lated as

$$\eta = \left(\frac{I - A}{2} \right) = -\frac{1}{2} (E_{\text{HOMO}} - E_{\text{LUMO}}). \quad (2)$$

The global softness (σ) describes the capacity of an atom or a group of atoms to receive electrons [21] and is equal to reciprocal of global hardness

$$\sigma = \frac{1}{\eta} = -\frac{2}{(E_{\text{HOMO}} - E_{\text{LUMO}})}. \quad (3)$$

Electronegativity (χ) is a measure of the power of an atom or a group of atoms to attract electrons towards itself [22] and can be calculated from HOMO-LUMO as

$$\chi = \left(\frac{I + A}{2} \right) = -\frac{1}{2} (E_{\text{HOMO}} + E_{\text{LUMO}}). \quad (4)$$

Polarizabilities were calculated at the same level of theory using the standard GAUSSIAN-09W keyword "Polar" [23]. This keyword means that the polarizabilities were obtained analytically rather than by numerical differentiation.

The energy of an uncharged molecule under a weak, general electric field can be expressed by Buckingham type expansion [24–26]:

$$E = E_0 - \mu_i F_i - (1/2)\alpha_{ij} F_i F_j - (1/6)\beta_{ijk} F_i F_j F_k - (1/24)\gamma_{ijkl} F_i F_j F_k F_l - \dots \quad (5)$$

where E is the energy of a molecule under the electric field F , E_0 is the unperturbed energy of a free molecule, F_i is the vector component of the electric field in the i -th direction, and μ_i , α_{ij} , β_{ijk} , γ_{ijkl} are the dipole moment, linear polarizability, first-order hyperpolarizability, and second-order hyperpolarizability, respectively. Here, each subscript of i , j , k , and l denotes the indices of the Cartesian axes x , y , z , and a repeated subscript means a summation over the Cartesian indices x , y , z . The ground state dipole moment (μ), the mean polarizability ($\langle \alpha \rangle$), the anisotropy of the polarizability ($\langle \Delta \alpha \rangle$) and the mean first-order hyperpolarizability (β), using the x , y , z components they are defined as [27, 28]:

$$\mu = (\mu_x^2 + \mu_y^2 + \mu_z^2)^{1/2}, \quad (6)$$

$$\langle \alpha \rangle = \frac{\alpha_{xx} + \alpha_{yy} + \alpha_{zz}}{3}, \quad (7)$$

$$\langle \Delta \alpha \rangle = \left\{ \frac{1}{2} \left[(\alpha_{xx} - \alpha_{yy})^2 + (\alpha_{yy} - \alpha_{zz})^2 + (\alpha_{zz} - \alpha_{xx})^2 + 6(\alpha_{xy}^2 + \alpha_{xz}^2 + \alpha_{yz}^2) \right] \right\}^{1/2}, \quad (8)$$

$$\beta = \left[(\beta_{xxx} + \beta_{xyy} + \beta_{xzz})^2 + (\beta_{yyy} + \beta_{yzz} + \beta_{yxx})^2 + (\beta_{zzz} + \beta_{zxx} + \beta_{zyy})^2 \right]^{1/2}. \quad (9)$$

The mean polarizability and mean first-order hyperpolarizability tensors ($\alpha_{xx}\alpha_{xy}$, α_{yy} , α_{xz} , α_{yz} , α_{zz} , and β_{xxx} , β_{xxy} , β_{xyy} , β_{yyy} , β_{xxz} , β_{xyz} , β_{yyz} , β_{zzz}) can be obtained by frequency job output file of GAUSSIAN-09W [12]. Since the values of the mean polarizabilities (α) and mean first-order hyperpolarizabilities (β) of GAUSSIAN-09W output are reported in atomic units (a.u.), the calculated values have been

converted into electrostatic units (esu) (α : 1 a.u. = 0.1482×10^{-24} esu; β : 1 a.u. = 8.6393×10^{-33} esu) [29].

3. Results and discussion

3.1. Electronic properties

The total energies and relative total energies of azo and hydrazone tautomers of (1) and (2) molecules calculated at B3LYP/6-31G(d,p) and B3LYP/aug-cc-pVDZ levels of theory are given in Table I. The total energy has also influence on the stability of a molecule. The total energies of (1) molecule have been calculated using B3LYP/6-31G(d,p) and B3LYP/aug-cc-pVDZ levels as -1062.5796 and -1062.5629 a.u. for hydrazone forms (-3633.6815 and -3636.1184 a.u. for hydrazone forms of (2) molecule) and -1062.5744 and -1062.5491 a.u. for azo forms (-3633.6770 and -3636.1031 a.u. for azo forms of (2) molecule), respectively. These results indicate that the hydrazone forms of (1) and (2) compounds are more stable than azo forms in gas phase.

TABLE I

Total energy (in a.u.), the relative total energies (in kcal/mol), E_{HOMO} , E_{LUMO} , $\Delta E_{\text{LUMO-HOMO}}$, ionization potential (I), electron affinity (A), molecular hardness (η), electronegativity (χ) (in eV) and molecular softness (σ) [eV^{-1}] values of (1) and (2) tautomers obtained by B3LYP/6-31G(d,p) and B3LYP/aug-cc-pVDZ levels.

	(1)		(2)	
	Azo form	Hydrazone form	Azo form	Hydrazone form
total energy ^a	-1062.5744	-1062.5796	-3633.6770	-3633.6815
total energy ^b	-1062.5491	-1062.5629	-3636.1031	-3636.1184
ΔE^a	3.26	0.00	2.82	0.0000
ΔE^b	8.66	0.00	9.60	0.0000
E_{HOMO}	-5.987	-6.055	-6.064	-6.135
E_{LUMO}	-3.349	-2.609	-3.495	-2.781
$\Delta E_{\text{LUMO-HOMO}}$	2.6374	3.4466	2.5682	3.3533
I	5.9873	6.0559	6.0641	6.1351
A	3.3499	2.6093	3.4959	2.7818
η	1.3187	1.7233	1.2841	1.6767
σ	0.7583	0.5803	0.7788	0.5964
χ	4.6686	4.3326	4.7800	4.4585

^a Total energies [a.u.] and the relative total energies [kcal/mol] obtained by B3LYP/6-31G(d,p) level.

^b Total energies [a.u.] and the relative total energies [kcal/mol] obtained by B3LYP/aug-cc-pVDZ level.

E_{HOMO} and E_{LUMO} refer to the highest occupied molecular orbital and lowest unoccupied molecular orbital energies, respectively. The HOMO (ability to donate an electron) implies the outermost orbital filled by electrons and is directly related to the ionization potential while the LUMO (ability to obtain an electron) can be thought as the first empty innermost orbital unfilled by electron and is directly related to the electron affinity. The HOMO and LUMO are called as the frontier molecule orbitals (FMOs). The HOMO-LUMO 3D orbital pictures computed at the B3LYP/6-31G (d,p) level for the title compounds are given in Fig. 2. The positive and negative phases are represented in red and green colour, respectively. As seen from Fig. 2, the LUMOs of both azo and hydrazone tautomers of (1) and (2)

molecules are largely delocalized almost over the whole molecular moiety but the HOMOs of both tautomers are mainly delocalized on the whole of tautomeric structures except phenyl rings.

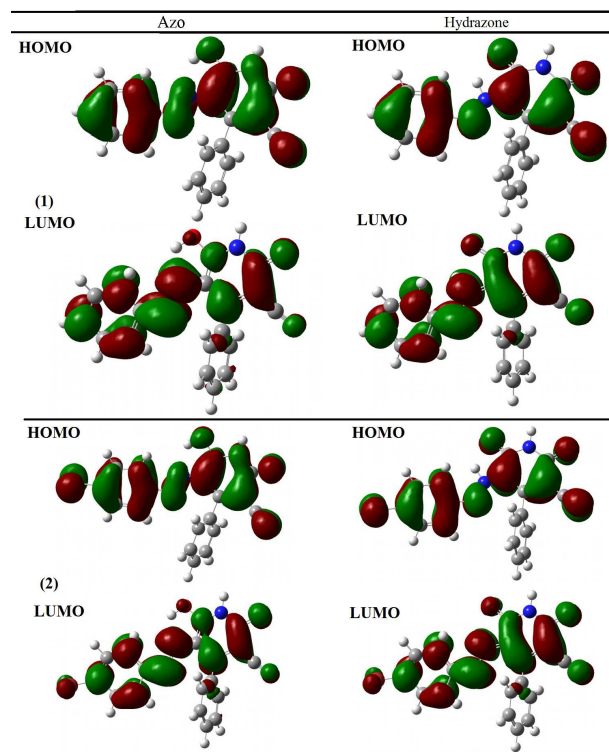


Fig. 2. The 3D plots frontier orbital energies for the azo and hydrazone tautomers of (1) and (2) compounds obtained by B3LYP/6-31G(d,p) level.

The calculated values for the E_{HOMO} and E_{LUMO} and the frontier molecular orbital energy gap ($\Delta E_{\text{LUMO-HOMO}}$) with B3LYP/6-31G(d,p) method are given in Table I. There are the formed energy gaps between the HOMO and LUMO. The frontier orbital gap helps to characterize the chemical reactivity and kinetic stability of the molecule. Meanwhile, a molecular with a small frontier orbital gap is more polarizable and is generally associated with a high chemical reactivity, low kinetic stability and is also termed as soft molecule [30, 31]. E_{HOMO} and E_{LUMO} of (1) have been calculated using B3LYP/6-31G(d,p) level as -6.0559 eV and -2.6093 eV (-6.1351 eV and -2.7818 eV of (2)) for hydrazone form and -5.9873 eV and -3.3499 eV (-6.0641 eV and -3.4959 eV of (2)) for azo form, respectively. The calculated values of the frontier orbital energy gap for (1) and (2) are 3.4466 and 3.3533 eV for hydrazone form and 2.6374 and 2.5682 eV for azo form, respectively (Table I).

The calculations of the frontier molecular orbital energy gaps for the (1) and (2) compounds using the B3LYP/6-31G(d,p) method indicate that the $\Delta E_{\text{LUMO-HOMO}}$ values between the LUMO and HOMO

orbital energies obtained for the hydrazone forms of (1) and (2) compounds, respectively (3.4466 and 3.3533 eV) are relatively higher than their values in the azo forms (2.6374 and 2.5682 eV). This indicates that the electron transfer from the HOMO orbital to the LUMO orbital is easier in the azo form for both compounds. Therefore, the hydrazone forms of (1) and (2) compounds are more stable than azo form of (1) and (2) compounds.

3.2. Molecular geometry

The arylazo pyridone dyes (1) and (2) having the same pyridone skeleton investigated in this work may exist in two tautomeric forms (Fig. 1). Depending on the tautomers, two types of intramolecular hydrogen bonds are observed in arylazo pyridone dyes: O–H···N in azo and N–H···O in hydrazone tautomers. The optimized molecular structures for the azo and hydrazone tautomers of the arylazo pyridone dyes (1) and (2) using the B3LYP/6-

31G(d,p) method are shown in Fig. 3a,b. Many researchers have studied the azo-hydrazone forms of arylazo pyridone dyes [32–34]. Table II composes the optimized structural parameters such as bond lengths and dihedral angles obtained only by geometrical optimization — since no experimental geometrical data are available in the literature — for the azo and hydrazone tautomers of (1) and (2) molecules by performing B3LYP with 6-31G(d,p) basis set. DFT calculations for the azo-hydrazone tautomers of dye (1) and the experimental structures of the arylazo pyridone dyes (1) and (2) have been reported by Alimmari et al. [11]. But the theoretical and experimental geometric data have not been given in that paper. Therefore we have compared the calculated structural parameters of the arylazo pyridone dyes (1) and (2) with experimentally available parent compound 2-pyridone from the X-ray study [35] and M06-2X/6-31+G(d,p) values obtained by Dostanić et al. [32].

TABLE II

Experimental and calculated bond lengths and dihedral angles at M06-2X/(6-31+G(d,p)) [32] and B3LYP/6-31G(d,p) methods for tautomeric forms of the (1) and (2) compounds.

Bond lengths	X-ray [35]	M06-2X/(6-31+G(d,p)) [32]				B3LYP/6-31G(d,p)			
		Substituents(R)		Substituents(R)		Substituents(R)		Substituents(R)	
		H	Br	H	Br	H	Br	H	Br
		(1)	(2)	(1)	(2)	(1)	(2)	(1)	(2)
		Azo	Hydrazo	Azo	Hydrazo	Azo	Hydrazo	Azo	Hydrazo
R–C10	–	1.085	1.087	1.881	1.882	1.086	1.085	1.907	1.903
C7–N1	1.39(2)	1.416	1.408	1.414	1.406	1.413	1.397	1.411	1.394
N1–N2	1.31(2)	1.263	1.292	1.264	1.294	1.264	1.282	1.265	1.284
N2–C5	1.32(1)	1.376	1.318	1.375	1.315	1.394	1.359	1.392	1.358
C5–C6	1.48(2)	1.410	1.472	1.410	1.474	1.404	1.469	1.405	1.470
C6–O1	1.19(2)	1.300	1.231	1.301	1.230	1.326	1.236	1.326	1.236
C5–C4	1.45(2)	–	–	–	–	1.435	1.426	1.436	1.426
N3–C6	1.40(1)	–	–	–	–	1.342	1.373	1.342	1.373
N3–C2	1.33(2)	–	–	–	–	1.419	1.404	1.420	1.404
C3–C4	1.37(2)	–	–	–	–	1.391	1.386	1.391	1.386
C3–C13	1.45(2)	–	–	–	–	1.429	1.426	1.429	1.426
C4–C14	1.52(2)	–	–	–	–	1.493	1.494	1.493	1.494
C2–O2	1.23(1)	–	–	–	–	1.218	1.219	1.218	1.219
C3–C2	1.47(2)	–	–	–	–	1.464	1.476	1.464	1.477
O–H···N	–	–	–	–	–	1.968	–	1.976	–
N–H···O	1.61(6)	–	–	–	–	–	1.982	–	1.977
corr. coefficient						0.79	0.95	0.79	0.95
Dihedral angles									
C7–N1–N2–C5	179.36					179.30	177.34	179.29	177.37
N1–N2–C5–C6						171.20	174.79	171.77	174.83
N1–N2–C5–C4	179.56					-7.32	-3.54	-6.78	-3.53
N2–C5–C6–O1						1.62	2.72	1.60	2.73

Firstly, by analyzing the dihedral angles around N–N moiety, all atoms of around N1–N2 of (1) and (2) compounds form nearly a planar molecule according to DFT calculation (Table II), as also supported by reported X-ray analysis result [35] with the torsion angle of 179.36° (C–N–N–C). From the values of N1–N2–C5–C4

dihedral angle calculated with B3LYP/6-31G(d,p) level in Table II, it can be seen that the arylazo pyridone ring is found -7.32° and -3.54° (in the azo and hydrazone structures, respectively) for (1) compound and -6.78° and -3.53° out of plane (in the azo and hydrazone structures, respectively) for (2) compound. An im-

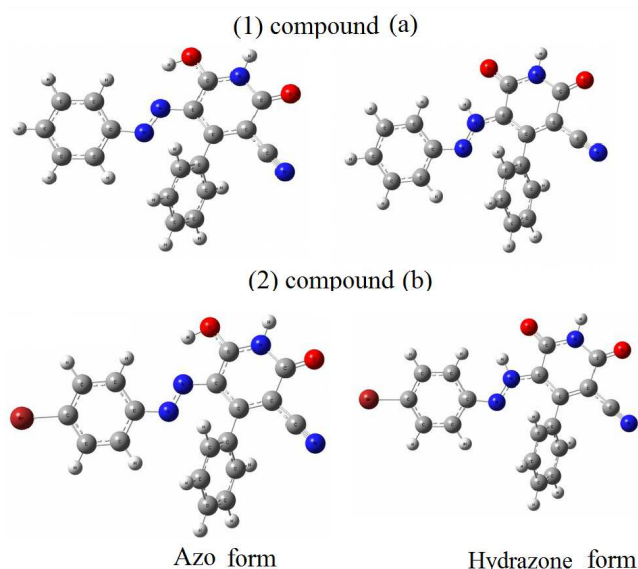


Fig. 3. (a) and (b) Tautomeric equilibria between azo and hydrazone forms, respectively, of the (1) and (2) compounds, (c) and (d) optimized structures between azo and hydrazone forms, respectively, of (1) and (2) compounds obtained using B3LYP/6-31G(d,p) level.

portant feature of the molecules is the strong intramolecular hydrogen bond formed between the hydrogen H(N2) and the 6-carbonyl group. The predicted O–H...N (azo) and N–H...O (hydrazone) distances for the compounds (1) and (2), respectively, are 1.968 and 1.976 Å for the azo tautomer, and 1.982 Å and 1.977 Å for the hydrazone tautomer (with B3LYP/6-31G(d,p)). These distances are significantly smaller than the summation of the Van der Waals radii (2.6 Å), just confirming the presence of a very strong hydrogen interaction in these compounds [6, 37]. The N₂...O distance is approximately 2.60 Å for (1) and (2) compounds, which is smaller than those intramolecular hydrogen bond, N⁻...O=C, in molecules that do not present electronic configuration (the N...O distance varies from 2.996 to 3.210 Å [38]).

The calculated N–N and C–N bond lengths of these compounds are also presented in Table II. As can be seen from Table II, from the crystalline structure described for parent compound 2-pyridone, the N–N bond length was 1.31(2) Å [35]. The calculated N–N bond distances were 1.264 Å and 1.265 Å for azo tautomer, whereas the N–N bond distance for the hydrazone isomer was 1.282 and 1.284 Å (at R–H and RBr substituents, respectively). The N1–N2 bond lengths calculated for azo form of (1) and (2) compounds are longer than average N=N distance for structural fragment C_{ar}–N = N–C_{ar} [39], but still not long enough to be considered as N_{sp2}–N_{sp2} standard single bond length (1.401 Å). This suggests a considerable electron delocalization on the azo linkage. In hydrazone form the N1–N2 bond length values are shorter than N_{sp2}–N_{sp2} single bond, which suggests a partially double bond character of it. The shortening of the hydrazone bond is related to the conjugation of N1–N2 bond with pyridone or benzene ring.

The calculated C–N bond lengths for these arylazo pyridone dyes compared with those corresponding to data reported in the literature [32]. These results from Table II clearly show that the bond lengths C7–N1 (1.413 and 1.397 of (1) compound and 1.411 and 1.394 of (2) compound for azo and hydrazone form, respectively) between benzene ring and azo bond fall between single C–N (1.431) and double C=N (1.279) bond, but have more single character in all forms. As shown in Table II, the calculated values with B3LYP/6-31G(d,p) level correspond well to those within the literature [32].

The N2–C5 bond lengths for (1) and (2) compounds have single-double character, which indicates resonance character between N1–N2 bond and the aromatic ring. This bond has more single character in azo form (1.394 for (1) and 1.392 for (2)), and more double character in hydrazone form (1.359 for (1) and 1.358 for (2)).

While the optimized C–C bonds of the rings for (1) and (2) compounds lie in the range of 1.391–1.493 Å for azo form and 1.386–1.494 Å for hydrazone form, the experimental values observed in the range of 1.37(2)–1.52(2) Å.

The C=O distances of both (1) and (2) were found 1.326 Å for azo form and 1.236 Å for hydrazone form. The short C=O distance (1.236 Å) for hydrazone form was nearer the C=O distance of 1.23 Å for the carbonyl group than the C–O distance (1.35 Å) found in phenols [40].

The data given in Table II obviously showed that the magnitude of the bond length was affected by substituent type. Structural analysis also revealed that the length of the bond that connects substituent R and benzene ring, R–C10, is almost the same in azo (1.085 Å, 1.086 Å for (1) and 1.881 Å, 1.907 Å for (2), Ref. [32] and B3LYP/6-31G(d,p), respectively) and hydrazone (1.087 Å, 1.085 Å for (1) and 1.882, 1.903 Å for (2), Ref. [32] and B3LYP/6-31G(d,p), respectively) forms compared with those corresponding to data reported in the literature [32].

For comparison with the experimental parameters, the calculated correlation (R^2) coefficients obtained with B3LYP/6-31G(d,p) level for the azo and hydrazone tautomers of the arylazo pyridine dyes (1) and (2) were shown in Fig. 4. We can see in Table II that the bond lengths

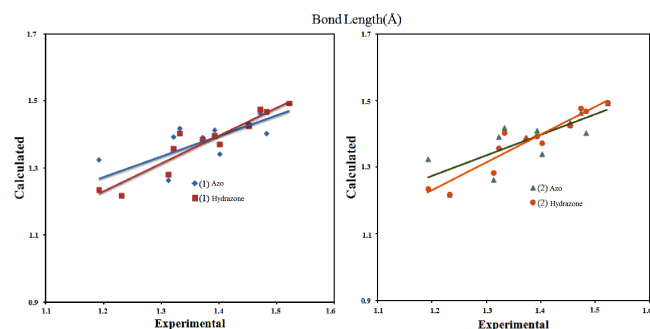


Fig. 4. Correlation graphics of experimental [35] and theoretical (with 6-31G(d,p)) bond lengths of the (1) and (2) compounds.

calculated by using the B3LYP methods with 6-31 G(d,p) basis set for the azo and hydrazone form of (1) and (2) compounds correlate fairly with experimental data (R^2 is both 0.79 for azo isomers and 0.95 for hydrazone isomers). According to B3LYP/6-31G(d,p) method, bond lengths of (1) and (2) compounds in hydrazone form give satisfactory result (linear correlation coefficients are $R^2 = 0.95$). For azo forms, the correlation coefficients obtained at B3LYP/6-31G(d,p) are both 0.79. The reason for this is that the azo tautomers are lower stability than the hydrazone forms thus are much lower percentage.

3.3. Global reactivity descriptors

Development of new chemical reactivity descriptors has gained significant momentum due to their applications in various areas of chemistry, biology, rational drug design and computer-aided toxicity prediction [41]. The understanding of chemical reactivity and selectivity of the molecular systems has been effectively handled by the conceptual DFT [42]. Global hardness (η), global softness (σ) and electronegativity (χ) are global reactivity descriptors, highly successful in predicting global chemical reactivity trends.

Associated within the framework of self-consistency function (SCF), MO theory, the ionization potential (I) and electron affinity (A) can be expressed through E_{HOMO} and E_{LUMO} orbital energies as $I = -E_{\text{HOMO}}$ and $A = -E_{\text{LUMO}}$. The obtained values of I and A were considered with most popularly used formulae for the computation of global hardness, global softness and electronegativity. Various reactivity descriptors as global hardness (η), global softness (σ) and electronegativity (χ) were evaluated using the standard working Eqs. (1)–(4) and these values calculated with B3LYP/6-31 G(d,p) level were listed in Table II. The global hardness (η) and global softness (σ) correspond to the gap between the E_{HOMO} and E_{LUMO} orbital energies and have been associated with the stability of chemical system. A soft molecule has a small energy gap and is more reactive than a hard one because it could easily offer electrons to an acceptor. The calculations with B3LYP/6-31G(d,p) method show that the global hardness (η) values of hydrazone tautomers for both molecules are greater than azo forms, and the global softness values of hydrazone tautomers are smaller than azo forms. This means that azo tautomers for both molecules have the largest potential chemical resistance to change the number of electrons among the other tautomers. Besides, these results indicate that hydrazone tautomers for both molecules are more stable than others in the gas phase.

3.4. Total electron density, molecular electrostatic potential, and electrostatic potential analyses

Molecular electrostatic potential (MEP), $V(r)$, at a given point $r(x, y, z)$ in the vicinity of a molecule, is defined in terms of the interaction energy between the electrical charge generated from the molecule's electrons and nuclei and a positive test charge (a proton) located

at r . For the system studied the $V(r)$ values were calculated as described previously using equation [43]:

$$V(r) = \sum_A \frac{Z_A}{(R_A - r)} - \int \frac{\rho(r')}{(r' - r)} dr', \quad (10)$$

where Z_A is the charge of nucleus A, located at R_A , $\rho(r')$ is the electronic density function of the molecule, and r' is the dummy integration variable.

MEP is typically visualized through mapping its values onto the surface reflecting the molecules boundaries. The different values of the MEP at the surface are represented by different colors; red, electron rich, partially negative charge; blue, electron deficient, partially positive charge; light blue, slightly electron deficient region; yellow, slightly electron rich region; and green, neutral. Potential increases in the order red < orange < yellow < green < blue. The molecular electrostatic potential is related to the electronic density and a very useful descriptor for determining sites for electrophilic attack and nucleophilic reactivities as well as hydrogen-bonding interactions [43, 44].

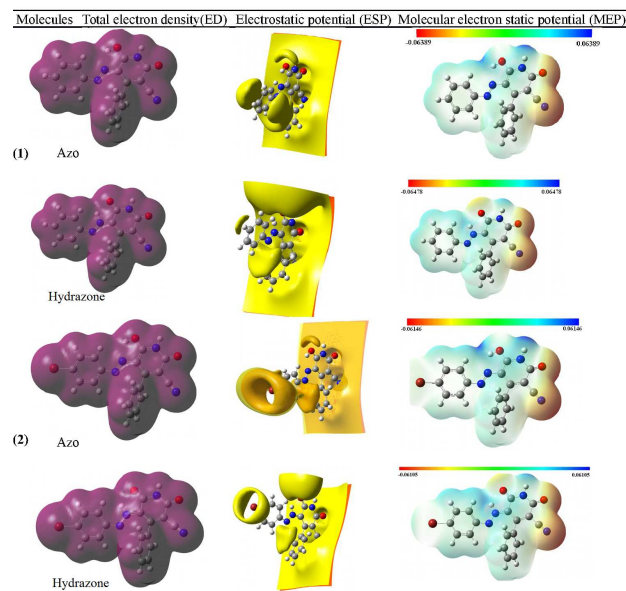


Fig. 5. The 3D plots of total ED, ESP, and MEP of (1) and (2) tautomers calculated at B3LYP/6-31G(d,p) level.

In the present study, the 3D plots of electrostatic potential (ESP), total electron density (ED) and MEP of (1) and (2) tautomers at B3LYP/6-31G(d,p) level are illustrated in Fig. 5. The ED plots for azo and hydrazone tautomers of (1) and (2) molecules show a uniform distribution. The MEP maps of (1) and (2) tautomers are shown in Fig. 5, where as electrophilic attack is presented by negative (red) regions, nucleophilic reactivity is shown by positive (blue) regions of MEP map of (1) and (2) tautomers. As seen from Fig. 5, the red regions are mainly localized on 3-cyano ($\text{C}\equiv\text{N}$) and 2-pyridines group, showing most favorable site for electrophilic attack. On the

other hand, when focused on positive regions of the electrostatic potential, we found that the hydrogen atoms of 2-pyridones ring are surrounded by blue color, indicating that these sites are probably involved in nucleophilic processes.

It can be seen from the ESP figure (Fig. 5) that the negative ESP is localized more over the Br atom and 2-pyridines ring and is reflected as a yellowish blob and the positive ESP is localized on the rest of the molecules.

3.5. NLO properties

In order to investigate the relationship among molecular structure and NLO properties, the dipole moments (μ), the polarizabilities (α), the anisotropy of the polarizabilities ($\langle\Delta\alpha\rangle$) and the first-order hyperpolarizabilities (β) for azo and hydrazone forms of (1) and (2) molecules were calculated using the B3LYP/6-31G(d,p) basis set, based on the finite-field approach. The dipole moment (μ) in a molecule is an important property, which is mainly used to study the intermolecular interactions involving the non-bonded type dipole-dipole interactions, because the higher the dipole moment, the stronger the intermolecular interactions will be [45]. The dipole moments of (1) and (2) tautomers obtained using DFT calculations are summarized in Table III. The calculated dipole moments for hydrazone

TABLE III
Dipole moments μ (D), polarizabilities (α) (in a.u. and esu), the anisotropic of the polarizabilities ($\langle\Delta\alpha\rangle$) (in a.u.) and the first-order hyperpolarizabilities (in a.u. and esu) values obtained using B3LYP/6-31G(d,p) method for azo and hydrazone tautomers of (1) and (2) compounds.

form	(1)		(2)	
	azo	hydrazone	azo	hydrazone
μ [D]	8.4724	9.5352	6.6296	7.6384
$\langle\alpha\rangle$ [a.u.]	253.65	278.08	285.53	316.07
$\langle\alpha\rangle \times 10^{-24}$ [esu]	37.59	41.21	42.32	46.84
$\langle\Delta\alpha\rangle$ [a.u.]	238.56	313.38	306.20	397.14
β [a.u.]	1260.28	730.20	888.09	4575.34
$\beta_{\text{tot}} \times 10^{-30}$ [esu]	10.89	6.31	7.67	39.53
$\beta_{\text{tot}}/\beta_{\text{urea}}$	56	32	39	203

forms (9.5352 and 7.6384 D) of the (1) and (2) compounds, respectively, have higher values than azo forms (8.4724 and 6.6296 D). The polarizabilities (α), the anisotropy of the polarizabilities ($\langle\Delta\alpha\rangle$) and the first-order hyperpolarizabilities (β) for azo and hydrazone forms of (1) and (2) molecules using B3LYP/6-31G(d,p) level are listed in Table III. Softness and polarizability are assumed to be related: "a soft species is also more polarizable." Thus, a hard (soft) species is known to correspond to a low (high) value of the polarizability as well as a small (large) size [46]. As seen in Table III, hydrazone forms of (1) and (2) compounds are softer and more polarizable than azo forms of these compounds.

It is well known that the higher values of first-order hyperpolarizability are important for more active NLO

properties. Urea is one of the prototypical molecules used in the study of the NLO properties of molecular systems. Therefore it was used frequently as a threshold value for comparative purposes. Theoretically, the first-order hyperpolarizabilities for NH forms of the (1) and (2) compounds are of 32 and 203 times magnitude of urea (the β of urea is 0.1947×10^{-30} esu), respectively. We conclude that the title compounds are attractive objects for future studies of NLO properties.

3.6. Natural bond orbital analysis

The natural bonding orbital (NBO) analysis is a helpful tool for understanding of hydrogen bonding and delocalization of electron density from occupied Lewis-type (donor) NBOs to properly unoccupied non-Lewis type (acceptor) NBOs within the molecule [47]. The NBO analysis has been performed on NH tautomers of (1) and (2) compounds to elucidate the intramolecular charge transfer (ICT), rehybridization and delocalization of electron density within the molecules and is presented in Table IV. The second-order Fock matrix was performed to evaluate different types of donor-acceptor interactions and their stabilization energies in the NBO basis [48]. For each donor (i) and acceptor (j), the stabilization energy $E(2)$ associated with the delocalization $i \rightarrow j$ is determined as

$$E2 = \Delta E_{ij} = q_{ij} \frac{F_{(i,j)}^2}{\varepsilon_j - \varepsilon_i}, \quad (11)$$

where q_i is the donor-orbital occupancy, ε_j and ε_i are the energies of σ and σ^* NBO's and $F_{(i,j)}$ is the Fock matrix element between the natural bonding orbitals. In NBO analysis, the larger the $E(2)$ value shows the more intensive interaction between electron-donors and electron-acceptors, i.e. the more electrons donating tendency from electron donors to acceptors and greater the extent of conjugation of the whole system, the possible intensive interactions are given in Table V.

The NBO analysis for NH forms of (1) and (2) dyes have been performed on the some arylazo pyridone dyes using NBO 3.1 program [18] as implemented in the Gaussian 09 package at the B3LYP/6-31G(d,p) level. The most important interactions in the title molecules having lone pair LP(1) N3 with that of anti-bonding C_6O_1 and the lone pair LP(1) N3 with that of anti-bonding C_2-O_2 , and results the stabilization of 66.92 and 67.20 kJ/mol (for (1) and (2) molecules, respectively) and 49.69 and 49.48 kJ/mol (for (1) and (2) molecules, respectively), which donate larger delocalization. The maximum energy transfer occurs from LP(1) N3 to C_6O_1 and C_2-O_2 . From the NBO analysis (Table V), it is noted that the maximum occupancies 1.99424, 1.99462, 1.99516 are obtained for C_6-O_1 , C_2-O_2 , $C_{13}-N_4$, respectively. This shows a large amount of stabilization energy.

The NBO analysis have revealed some strong intramolecular interactions, which are formed by the orbital overlap between $\sigma(C-C)$ and $\sigma^*(C-C)$ and $\pi(C-C)$ and $\pi^*(C-C)$ bond orbital in the aromatic rings, which leads intramolecular charge transfer (ICT) to cause

NBO results showing the formation of Lewis and non-Lewis orbitals.

TABLE IV

			(1)					(2)				
			%	% <i>s</i>	% <i>p</i>	% <i>d</i>	H.O	%	% <i>s</i>	% <i>p</i>	% <i>d</i>	H.O
C ₁₁ -C ₁₀	σ	C ₁₁	50.19	35.17	64.79	0.04	<i>sp</i> ^{1.84}	49.38	34.50	65.46	0.04	<i>sp</i> ^{1.90}
		C ₁₀	49.81	34.92	65.04	0.04	<i>sp</i> ^{1.86}	50.62	38.87	61.09	0.04	<i>sp</i> ^{1.57}
	π	C ₁₁	-	-	-	-	-	47.08	0.00	99.95	0.04	<i>sp</i>
		C ₁₀	-	-	-	-	-	52.92	0.00	99.98	0.02	<i>sp</i>
C ₇ -N ₁	σ	C ₇	41.00	27.90	71.99	0.10	<i>sp</i> ^{2.58}	41.16	28.26	71.63	0.10	<i>sp</i> ^{2.53}
		N ₁	59.00	35.25	64.66	0.08	<i>sp</i> ^{1.83}	58.84	35.31	64.60	0.08	<i>sp</i> ^{1.83}
C ₉ -C ₁₀	σ	C ₉	50.09	35.04	64.92	0.04	<i>sp</i> ^{2.06}	49.28	34.37	65.59	0.04	<i>sp</i> ^{1.91}
		C ₁₀	49.91	35.06	64.90	0.04	<i>sp</i> ^{1.81}	50.72	39.04	60.92	0.04	<i>sp</i> ^{1.56}
C ₁₀ -Br	σ	C ₁₀	-	-	-	-	-	49.56	22.09	77.81	0.11	<i>sp</i> ^{1.91}
		Br	-	-	-	-	-	50.44	13.85	85.85	0.29	<i>sp</i> ^{6.20}
N ₁ -N ₂	σ	N ₁	45.37	27.55	72.31	0.13	<i>sp</i> ^{2.62}	45.41	27.57	72.30	0.13	<i>sp</i> ^{2.62}
		N ₂	54.63	33.84	66.10	0.06	<i>sp</i> ^{1.95}	54.59	33.87	66.07	0.06	<i>sp</i> ^{1.95}
	π	N ₁	42.71	0.12	99.60	2.24	<i>sp</i> ^{99.99} <i>d</i> ^{2.24}	-	-	-	-	-
		N ₂	57.29	0.11	99.80	0.08	<i>sp</i> ^{99.99} <i>d</i> ^{0.71}	-	-	-	-	-
N ₂ -C ₅	σ	N ₂	62.49	38.06	61.91	0.03	<i>sp</i> ^{1.63}	62.49	38.07	61.90	0.03	<i>sp</i> ^{1.63}
		C ₅	37.51	28.59	71.31	0.10	<i>sp</i> ^{2.49}	37.51	28.63	71.27	0.10	<i>sp</i> ^{2.49}
	π	N ₂	-	-	-	-	-	60.02	0.02	99.95	0.03	<i>sp</i> ^{99.99} <i>d</i> ^{1.57}
		C ₅	-	-	-	-	-	39.98	0.00	99.92	0.07	<i>sp</i>
C ₅ -C ₆	σ	C ₅	51.98	32.16	67.79	0.05	<i>sp</i> ^{2.11}	51.99	32.11	67.84	0.05	<i>sp</i> ^{2.11}
		C ₆	48.02	35.96	63.99	0.05	<i>sp</i> ^{1.78}	48.01	35.90	64.05	0.05	<i>sp</i> ^{1.78}
C ₅ -C ₄	σ	C ₅	49.97	39.18	60.79	0.03	<i>sp</i> ^{1.55}	49.99	39.19	60.79	0.03	<i>sp</i> ^{1.55}
		C ₄	50.03	32.39	67.56	0.04	<i>sp</i> ^{2.09}	50.01	32.33	67.62	0.04	<i>sp</i> ^{2.09}
C ₆ -O ₁	σ	C ₆	35.49	32.59	67.32	0.09	<i>sp</i> ^{2.07}	35.48	32.60	67.31	0.09	<i>sp</i> ^{2.06}
		O ₁	64.51	39.78	59.89	0.33	<i>sp</i> ^{1.51}	64.52	39.78	59.89	0.33	<i>sp</i> ^{1.51}
	π	C ₆	28.52	0.00	99.80	0.20	<i>sp</i>	28.56	0.00	99.80	0.20	<i>sp</i>
		O ₁	71.48	0.00	99.70	0.30	<i>sp</i>	71.44	0.00	99.70	0.30	<i>sp</i>
C ₆ -N ₃	σ	C ₆	37.68	31.25	68.64	0.12	<i>sp</i> ^{2.20}	37.70	31.31	68.58	0.12	<i>sp</i> ^{2.19}
		N ₃	62.32	36.77	63.19	0.03	<i>sp</i> ^{1.72}	62.30	36.77	63.20	0.03	<i>sp</i> ^{1.72}
C ₄ -C ₃	σ	C ₄	50.10	34.73	65.23	0.04	<i>sp</i> ^{1.88}	50.09	34.74	65.22	0.04	<i>sp</i> ^{1.88}
		C ₃	49.90	37.48	62.49	0.03	<i>sp</i> ^{1.67}	49.91	37.50	62.47	0.03	<i>sp</i> ^{1.67}
	π	C ₄	42.79	0.00	99.93	0.06	<i>sp</i>	42.97	0.00	99.93	0.06	<i>sp</i>
		C ₃	57.21	0.00	99.98	0.02	<i>sp</i>	57.03	0.00	99.98	0.02	<i>sp</i>
C ₄ -C ₁₄	σ	C ₄	51.48	32.85	67.11	0.03	<i>sp</i> ^{2.04}	51.51	32.90	67.06	0.03	<i>sp</i> ^{2.04}
		C ₁₄	48.52	30.21	69.75	0.04	<i>sp</i> ^{2.31}	48.49	30.19	69.77	0.04	<i>sp</i> ^{2.31}
C ₃ -C ₂	σ	C ₃	52.70	31.62	68.34	0.04	<i>sp</i> ^{2.16}	52.71	31.59	68.37	0.04	<i>sp</i> ^{2.16}
		C ₂	47.30	37.20	62.75	0.05	<i>sp</i> ^{1.69}	47.29	37.17	62.77	0.05	<i>sp</i> ^{1.69}
C ₃ -C ₁₃	σ	C ₃	51.49	30.87	69.09	0.05	<i>sp</i> ^{2.24}	51.51	30.87	69.08	0.05	<i>sp</i> ^{2.24}
		C ₁₃	48.51	52.47	47.50	0.04	<i>sp</i> ^{0.91}	48.49	52.45	47.52	0.04	<i>sp</i> ^{0.91}
C ₂ -N ₃	σ	C ₂	36.58	29.36	70.51	0.13	<i>sp</i> ^{2.40}	36.58	29.38	70.49	0.13	<i>sp</i> ^{2.40}
		N ₃	63.42	35.96	64.01	0.03	<i>sp</i> ^{1.78}	63.42	35.93	64.04	0.03	<i>sp</i> ^{1.78}
C ₂ -O ₂	σ	C ₂	35.31	33.24	66.67	0.09	<i>sp</i> ^{2.01}	35.31	33.25	66.66	0.09	<i>sp</i> ^{2.01}
		O ₂	64.69	41.04	58.60	0.36	<i>sp</i> ^{1.43}	64.69	41.05	58.59	0.36	<i>sp</i> ^{1.43}
	π	C ₂	32.03	0.00	99.83	0.17	<i>sp</i>	32.12	0.00	99.83	0.17	<i>sp</i>
		O ₂	67.97	0.00	99.67	0.33	<i>sp</i> ^{1.74}	67.88	0.00	99.67	0.33	<i>sp</i>
C ₁₃ -N ₄	σ	C ₁₃	42.53	47.64	52.34	0.02	<i>sp</i> ^{1.10}	42.54	47.65	52.32	0.02	<i>sp</i> ^{1.10}
		N ₄	57.47	45.88	53.78	0.34	<i>sp</i> ^{1.17}	57.46	45.85	53.81	0.34	<i>sp</i> ^{1.17}
	π	C ₁₃	46.52	0.03	99.92	0.05	<i>sp</i> ^{99.99} <i>d</i> ^{1.76}	46.54	0.03	99.92	0.05	<i>sp</i> ^{99.99} <i>d</i> ^{1.73}
		N ₄	53.48	0.01	99.61	0.38	<i>sp</i> ^{99.99} <i>d</i> ^{36.95}	53.46	0.01	99.61	0.38	<i>sp</i> ^{99.99} <i>d</i> ^{36.20}
	π ₂	C ₁₃	45.76	0.00	99.95	0.05	<i>sp</i>	45.84	0.00	99.95	0.05	<i>sp</i>
		N ₄	54.24	0.00	99.63	0.37	<i>sp</i>	54.16	0.00	99.63	0.37	<i>sp</i>
C ₁₄ -C ₁₉	σ	C ₁₄	51.46	34.79	65.17	0.03	<i>sp</i> ^{1.87}	51.47	34.80	65.17	0.03	<i>sp</i> ^{1.87}
		C ₁₉	48.54	34.69	65.27	0.04	<i>sp</i> ^{2.06}	48.53	34.68	65.28	0.04	<i>sp</i> ^{1.88}

The second-order perturbation theory analysis of Fock matrix in natural bond orbital (NBO basis) for the hydrate tautomer of (1) and (2) molecules.

Donor (i)	Type	ED(i)(e)		Acceptor (j)	Type	ED(j)(e)		E(2) ^a [kcal/mol]		$\varepsilon(j)-\varepsilon(i)^b$ [a.u.]		F(i,j) ^c [a.u.]	
		(1)	(2)			(1)	(2)	(1)	(2)	(1)	(2)	(1)	(2)
C ₁₁ -C ₁₂	σ	1.97810	1.97058	C ₇ -N ₁	σ^*	0.02284	0.02204	4.50	4.33	1.14	1.15	0.064	0.063
C ₁₁ -C ₁₀	σ	1.98120	1.98197	C ₁₁ -C ₁₂	σ^*	0.01447	0.01568	2.54	2.55	1.28	1.31	0.051	0.052
C ₁₂ -C ₇	σ	1.97885	1.97912	C ₇ -C ₈	σ^*	0.02234	0.02209	3.72	3.61	1.26	1.26	0.061	0.060
C ₇ -C ₈	σ	1.97296	1.97319	C ₁₂ -C ₇	σ^*	0.03231	0.03254	3.50	3.36	1.24	1.24	0.059	0.058
				N ₁ -N ₂		0.01818	0.01762	2.87	2.90	1.17	1.17	0.052	0.052
C ₇ -N ₁	σ	1.98107	1.98105	N ₂ -C ₅	σ^*	0.02575	0.02544	5.40	5.30	1.26	1.27	0.074	0.073
C ₈ -C ₉	σ	1.97984	1.97194	C ₇ -C ₈	σ^*	0.02234	0.02209	2.40	2.33	1.25	1.25	0.049	0.048
				C ₉ -C ₁₀		0.01552	0.02527	2.47	2.84	1.27	1.15	0.050	0.051
				C ₁₀ -Br			0.03026	-	4.67	-	0.80	-	0.055
	π	1.66282	1.66914	C ₁₁ -C ₁₀	π^*		0.39409	-	20.21	-	0.27	-	0.067
				C ₁₂ -C ₇			0.43158	-	18.96	-	0.27	-	0.066
C ₉ -C ₁₀	σ	1.98138	1.98213	C ₈ -C ₉	σ^*	0.01374	0.01491	2.49	2.50	1.28	1.31	0.050	0.051
C ₁₀ -Br	σ		1.98634	C ₁₁ -C ₁₂	σ^*	0.01447	0.01568	-	2.88	-	1.22	-	0.053
N ₁ -N ₂	σ	1.98883	1.98857	N ₂ -C ₅	σ^*	0.02575	0.02544	2.44	2.46	1.44	1.44	0.053	0.053
N ₂ -C ₅	σ	1.98341	1.98346	C ₇ -N ₁	σ^*	0.02284	0.02204	2.66	2.66	1.31	1.31	0.053	0.053
C ₅ -C ₆	σ	1.97026	1.97019	N ₁ -N ₂	σ^*	0.01818	0.01762	5.91	5.95	1.16	1.16	0.074	0.074
C ₅ -C ₄	σ	1.96945	1.96949	N ₂ -C ₅	σ^*	0.02575	0.02544	2.04	2.05	1.17	1.17	0.044	0.044
				C ₄ -C ₃		0.02936	0.02938	3.25	3.23	1.30	1.30	0.058	0.058
C ₆ -N ₃	σ	1.98789	1.98790	N ₂ -C ₅	σ^*	0.02575	0.02544	1.80	1.78	1.30	1.30	0.043	0.043
				C ₂ -O ₂		0.00849	0.00846	1.96	1.96	1.45	1.45	0.048	0.048
C ₄ -C ₃	σ	1.96405	1.96415	N ₂ -C ₅	σ^*	0.02575	0.02544	4.51	4.49	1.19	1.19	0.065	0.065
				C ₁₃ -N ₄		0.00964	0.00963	4.24	4.24	1.64	1.64	0.075	0.075
C ₄ -C ₃	π	1.76485	1.76469	C ₂ -O ₂		0.29077	0.28835	23.70	23.50	0.29	0.29	0.075	0.075
				C ₁₃ -N ₄	π_2^*	0.08638	0.08529	18.69	18.54	0.40	0.40	0.080	0.080
C ₄ -C ₁₄	σ	1.96772	1.96771	C ₄ -C ₃	σ^*	0.02936	0.02938	3.41	3.44	1.23	1.23	0.058	0.058
				C ₃ -C ₂		0.07231	0.07251	3.49	3.50	1.09	1.09	0.056	0.056
C ₃ -C ₂	σ	1.96832	1.96838	C ₄ -C ₁₄	σ^*	0.03052	0.03056	3.30	3.31	1.13	1.13	0.054	0.055
				C ₁₃ -N ₄		0.00964	0.00963	3.90	3.89	1.59	1.59	0.071	0.070
				C ₁₃ -N ₄	π^*	0.01516	0.01513	2.55	2.55	0.81	0.81	0.041	0.041
C ₃ -C ₁₃	σ	1.97743	1.97742	C ₂ -N ₃	σ^*	0.08752	0.08759	2.65	2.65	1.13	1.13	0.050	0.050
				C ₁₃ -N ₄		0.00964	0.00963	5.96	5.96	1.63	1.63	0.088	0.088
C ₂ -N ₃	σ	1.98760	1.98759	C ₆ -O ₁	σ^*	0.01013	0.01015	2.97	2.99	1.37	1.37	0.057	0.057
C ₆ -O ₁		1.99424		C ₆ -N ₃	σ^*	0.07121	-	1.74	-	1.47	-	0.046	-
C ₂ -O ₂	σ	1.99462	1.99463	C ₆ -N ₃	σ^*	0.07121	0.07099	1.67	1.67	1.51	1.51	0.046	0.046
C ₁₃ -N ₄	σ	1.99516	1.99515	C ₃ -C ₁₃	σ^*	0.02849	0.02851	6.46	6.46	1.55	1.55	0.090	0.090
C ₁₃ -N ₄	π_2	1.95219	1.95119	C ₄ -C ₃	π^*	0.28820	0.28498	8.76	8.84	0.33	0.33	0.051	0.052
LP(1) N1		1.92940	1.92925	C ₁₂ -C ₇	σ^*	0.03231	0.03254	8.04	8.38	0.95	0.94	0.079	0.080
LP(2) N1			-	C ₁₂ -C ₇	π^*		0.43158	-	42.60	-	0.22	-	0.097
LP(2) N1			-	N ₂ -C ₅	π^*		0.69873	-	100.06	-	0.14	-	0.111
LP(1) O1		1.97439	1.97435	C ₅ -C ₆	σ^*	0.06479	0.06506	3.61	3.62	1.12	1.12	0.057	0.057
LP(2) O1		1.84682	1.84634	C ₅ -C ₆		0.06479	0.06506	17.13	17.15	0.70	0.70	0.100	0.100
				C ₆ -N ₃		0.07121	0.07099	24.86	24.83	0.72	0.72	0.122	0.122
LP(1) N3		1.62906	1.62850	C ₆ -O ₁	π^*	0.37347	0.37208	66.92	67.20	0.26	0.26	0.118	0.119
				C ₂ -O ₂		0.29077	0.28835	49.69	49.48	0.29	0.29	0.108	0.108
LP(1) N4		1.96925	1.96925	C ₃ -C ₁₃	σ^*	0.02849	0.02851	12.87	12.89	1.02	1.02	0.103	0.103
LP(2) O2		1.85715	1.85693	C ₃ -C ₂		0.07231	0.07251	21.05	21.12	0.68	0.68	0.109	0.109
				C ₂ -N ₃		0.08752	0.08759	28.61	28.66	0.66	0.66	0.124	0.124
LP(2) Br			1.97497	C ₁₁ -C ₁₀		0.01545	0.02526	-	3.07	-	0.84	-	0.045

^a E(2) means energy of hyperconjugative interactions, ^b Energy difference between donor and acceptor *i* and *j* NBO orbitals, ^c F_{ij} is the Fock matrix element between *i* and *j* NBO orbitals.

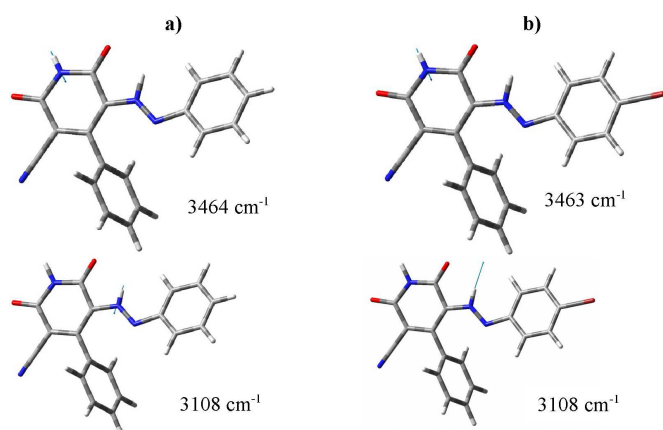


Fig. 7. Vector representation for the main infrared active normal modes calculated at B3LYP/6-31G(d,p) level for the hydrazone species of (a) (1) and (b) (2) compounds.

basis set, respectively. This stretching has been observed at 3439 cm^{-1} [11]. In the present investigation, the N–H stretching vibrations of hydrazone tautomeric forms have been found very weak band at 3170 cm^{-1} . The calculated N–H stretching vibrations for hydrazone tautomers of (1) and (2) compounds (see Fig. 6) are both at 3108 cm^{-1} using B3LYP methods with 6-31G(d,p) basis set. These N–H vibrations of hydrazone tautomers are most pure mode as evidenced from 98% of PED in (1) and (2) compounds.

3.7.2. C–H vibrations

The hetero aromatic structure shows the presence of C–H stretching vibrations in the region $3100\text{--}3000\text{ cm}^{-1}$ which is the characteristic region for the ready identification of C–H stretching vibrations [50]. The B3LYP/6-31G(d,p) calculations give bands in the range $3096\text{--}3054\text{ cm}^{-1}$ and $3102\text{--}3058\text{ cm}^{-1}$ for (1) and (2) compounds, respectively, as m(CH) modes. As indicated by PED, these modes involve exact contribution of $> 92\%$ suggesting that they are pure stretching modes. In this region, the bands are not affected remarkably by the nature of the substituent.

The C–H out of plane deformation is observed between 1000 and 700 cm^{-1} [51]. The calculated out of plane bending vibrations at B3LYP method give the mode at $745, 753, 808, 822, 895, 933, 940, 962\text{ cm}^{-1}$ ($748, 793, 821, 823, 895, 932, 934, 951, 962\text{ cm}^{-1}$ for (2) compound) for (1) compound.

3.7.3. C=N and C≡N vibrations

The bands in the region of $1300\text{--}1200\text{ cm}^{-1}$ are due to C=N stretching vibrations, which shift the wave number and intensity in a coordination compound fashion depending on the neighbouring group, conjugation effects, H-bonding and molecular tautomerism [52]. The bands appearing in the IR spectrum at $1447, 1395, 1270,$ and 1202 cm^{-1} correspond to the stretching vibrations of the C=N group. The calculated bands are 1455 (15%), 1382 (12%), 1265 (12%) and 1214 (29%) cm^{-1} ($1453, 1381, 1266$ and 1215 cm^{-1} for (2) compound) at the B3LYP/6-31G(d,p) level for the C=N vibrational modes. The ob-

tained results are consistent with the previous report concerning 5-(4-, 3- and 2-methoxyphenylazo)-3-cyano-1-ethyl-6-hydroxy-4-methyl-2-pyridone [31].

Unsaturated or aromatic nitriles, in which the double bond or ring is adjacent to the C≡N group, absorbs more strongly in the infrared than saturated compounds, and the related band occurs at somewhat lower frequency near 2230 cm^{-1} [53]. In our present work, theoretically computed value (ν_{15}) is assigned to the stretching of C≡N group which is contributing to 89% of PED, and it is in a good agreement with our experimental spectrum; the observed band in FT-IR spectrum is at 2224 cm^{-1} . The vibrational modes (ν_{15}), which are calculated at 2249 cm^{-1} for (1) and (2) compounds are assigned to the in-plane stretching vibration of C≡N group.

3.7.4. C=O vibrations

The structural unit of carbonyl (C=O) has an excellent group frequency which is described as a stretching vibration, and this group has been most extensively studied by infrared spectroscopy. Compounds containing the carbonyl group present a very intense and narrow peak in the infrared region, placed within $1800\text{--}1600\text{ cm}^{-1}$, referring to the stretching vibration of the C=O bond, $\nu(\text{C=O})$. The double bond between the carbon–oxygen atoms is formed by $\pi\text{--}\pi$ bonding between carbon and oxygen. Because these atoms have different electronegativities, the bonding electrons are not equally distributed between the two atoms [54]. The calculated absorptions at ≈ 1715 (84%) and ≈ 1686 (67%) cm^{-1} for hydrazone forms of both compounds by B3LYP/6-31G(d,p) method are modes 16 and 17, respectively, which belongs to the stretching of bond C=O of pyridine ring.

3.7.5. C–Br vibrations

Bromine compounds absorb strongly in the region $650\text{--}450\text{ cm}^{-1}$ due to the CBr stretching vibrations [55]. In the spectra of (2) molecule the $\nu(\text{C–Br})$ stretching vibration contributes to the bands computed at $333, 540,$ and 1048 cm^{-1} (which is contributing to 24, 12 and 12%, respectively) by B3LYP/6-31G(d,p) method (modes 96, 84, and 50, respectively, in Table VI). These results show excellent agreement with the assignment reported earlier [56]. According to the calculated PED, the out-of-plane $\gamma(\text{C–Br})$ bending vibration in (2) should be assigned to the band at 330 (mode 97).

4. Conclusions

The molecular structures and quantum chemical parameters for the hydrazone and azo forms of (1) and (2) dyes were studied using B3LYP method at 6-31G(d,p) basis set. Calculated results reveal that the hydrazone form of (1) and (2) compounds are more stable than azo form in gas phase. NLO behaviors for the azo and hydrazone forms of (1) and (2) molecules were investigated by determining the dipole moment $\mu(\text{D})$, the polarizability $\langle\alpha\rangle$ (in a.u. and esu), the anisotropic of the polarizabilities $\langle\Delta\alpha\rangle$ (in a.u.) and the first-order

TABLE VI

Comparison of the experimental FT-IR wave numbers [cm^{-1}] for (2) compound and theoretical harmonic wave numbers [cm^{-1}] for hydrazone tautomer of (1) and (2) by B3LYP/6-31G(d,p) method.

ν	Assignments (%PED ^d)	Expt ^a	(1)				(2)			
			A ^b	B ^c	IR int.	R act.	A ^b	B ^c	IR Int.	R act.
1	$\nu(\text{NH})_{\text{pyr}}$ (100)	3439	3605	3464	97	187	3604	3463	102	198
2	$\nu(\text{NH})$ (98)	3170	3236	3108	46	420	3236	3108	46	753
3	$\nu(\text{CH})_{\text{ph1}}$ (98)		3222	3096	11	164	3229	3102	3	133
4	$\nu(\text{CH})_{\text{ph1}}$ (95)		–	–	–	–	3224	3098	2	134
5	$\nu_{\text{as}}(\text{CH})_{\text{ph1}}$ (99)		3213	3087	22	389	3216	3090	1	56
6	$\nu(\text{CH})_{\text{ph2}}$ (95)		3213	3087	11	269	3213	3087	11	251
7	$\nu_{\text{as}}(\text{CH})_{\text{ph2}}$ (92)		3205	3079	22	27	3205	3079	21	27
8	$\nu_{\text{as}}(\text{CH})_{\text{ph1}}$ (84)		3202	3076	11	189	–	–	–	–
9	$\nu_{\text{as}}(\text{CH})_{\text{ph2}}$ (92)		3198	3073	13	78	3198	3073	12	79
10	$\nu_{\text{as}}(\text{CH})_{\text{ph1}}$ (89)	3036	3194	3069	2	64	–	–	–	–
11	$\nu_{\text{as}}(\text{CH})_{\text{ph2}}$ (94)	2924	3190	3065	1	98	3190	3065	1	95
12	$\nu_{\text{as}}(\text{CH})_{\text{ph1}}$ (96)		–	–	–	–	3186	3061	3	32
13	$\nu_{\text{as}}(\text{CH})_{\text{ph2}}$ (97)		3183	3058	1	23	3183	3058	1	21
14	$\nu_{\text{as}}(\text{CH})_{\text{ph1}}$ (98)	2853	3179	3054	4	28	–	–	–	–
15	$\nu(\text{C}\equiv\text{N})$ (89), $\nu_{\text{as}}(\text{CC})_{\text{pyr}}$ (11)	2224	2341	2249	37	1431	2341	2249	37	1809
16	$\nu(\text{C}=\text{O})$ (84)	1697	1785	1715	622	441	1786	1716	653	612
17	$\nu(\text{C}=\text{O})$ (67)	1652	1755	1686	339	53	1756	1688	329	75
18	$\nu(\text{CC})_{\text{ph2}}$ (50)		1659	1594	1	50	1659	1594	1	50
19	$\nu(\text{CC})_{\text{ph1}}$ (49), $\nu(\text{NN})$ (10)		1655	1590	51	625	1644	1580	221	1065
20	$\nu_{\text{as}}(\text{CC})_{\text{ph2}}$ (55)	1513	1635	1571	3	12	1635	1571	4	15
21	$\nu_{\text{as}}(\text{CC})_{\text{ph1}}$ (35)		1628	1564	14	683	1610	1547	45	3722
22	$\nu_{\text{as}}(\text{CC})_{\text{ph1}}$ (24), $\delta(\text{NH})$ (20), $\nu(\text{N}-\text{N})$ (12)		1600	1537	267	2528	1594	1532	153	2189
23	$\nu(\text{CC})_{\text{pyr}}$ (48)		1559	1498	73	1433	1560	1499	83	2656
24	$\nu(\text{CC})_{\text{ph2}}$ (15), $\delta(\text{CCH})_{\text{ph2}}$ (35)		1535	1475	217	982	1535	1475	217	1448
25	$\delta(\text{CCH})_{\text{ph1,ph2}}$ (46)		1530	1470	1	939	1526	1466	1	1158
26	$\nu_{\text{as}}(\text{CC})_{\text{pyr}}$ (19), $\nu(\text{N}=\text{C})$ (15)	1447	1514	1455	480	183	1512	1453	695	255
27	$\delta(\text{CCH})_{\text{ph1}}$ (23)		1494	1435	56	86	–	–	–	–
28	$\delta(\text{CCH})_{\text{ph2}}$ (52)	1410	1484	1426	39	53	1484	1426	41	61
29	$\nu(\text{CC})_{\text{ph1}}$ (41)		–	–	–	–	1453	1396	55	83
30	$\nu(\text{CC})_{\text{pyr}}$ (15), $\nu(\text{N}=\text{C})$ (12)	1395	1438	1382	316	256	1437	1381	338	523
31	$\nu(\text{N}-\text{N})$ (11), $\nu(\text{NC})$ (13), $\delta(\text{NH})$ (39)		1405	1350	277	257	1406	1351	318	776
32	$\delta(\text{NH})$ (51), $\nu(\text{N}-\text{N})$ (17)		1399	1344	196	2097	1399	1344	152	3400
33	$\nu_{\text{as}}(\text{CCH})_{\text{ph1}}$ (29), $\delta(\text{N}-\text{H})$ (46)		1370	1316	7	44	–	–	–	–
34	$\delta(\text{CCH})_{\text{ph2}}$ (12), $\delta(\text{CCH})_{\text{ph2}}$ (59)	1302	1361	1308	1	1	1361	1308	1	2
35	$\nu(\text{CC})_{\text{ph1}}$ (41)		1346	1293	58	5	1341	1288	88	26
36	$\delta(\text{CC})_{\text{ph1}}$ (25), $\delta(\text{CCH})_{\text{ph1}}$ (63)		–	–	–	–	1333	1281	3	47
37	$\delta(\text{CC})_{\text{ph2}}$ (39)		1332	1280	1	146	1331	1279	4	233
38	$\delta(\text{CC})_{\text{ph1,ph2,pyr}}$ (12), $\nu(\text{N}=\text{C})$ (12)	1270	1317	1265	9	1550	1318	1266	7	2670
39	$\nu(\text{N}=\text{C})$ (29)	1202	1264	1214	4	60	1265	1215	4	71
40	$\nu(\text{NC})$ (15), $\nu_{\text{as}}(\text{CC})_{\text{pyr}}$ (11)		1245	1196	1	1280	1247	1198	2	1768
41	$\sigma(\text{CH})_{\text{ph2}}$ (74)	1164	1210	1163	1	6	1210	1163	1	6
42	$\sigma(\text{CH})_{\text{ph1}}$ (61)		1206	1159	6	726	1205	1158	4	1622
43	$\sigma(\text{CH})_{\text{ph2}}$ (37)		1190	1143	0	6	1190	1143	0	9
44	$\nu_{\text{as}}(\text{CC})_{\text{pyr}}$ (10)		1161	1115	0	597	1162	1116	2	789
45	$\sigma(\text{CH})_{\text{ph1}}$ (42)		1142	1097	24	31	1144	1099	7	192
46	$\sigma(\text{CH})_{\text{ph1}}$ (11), $\nu_{\text{as}}(\text{CC})_{\text{pyr}}$ (39)		–	–	–	–	1141	1096	21	73
47	$\delta(\text{CCH})_{\text{ph2}}$ (40), $\nu(\text{CC})_{\text{pyr}}$ (34)	1068	1110	1066	4	3	1110	1066	4	4
48	$\nu(\text{CC})_{\text{ph1}}$ (54), $\nu(\text{BrC})$ (12)		–	–	–	–	1091	1048	104	391
49	$\nu(\text{CC})_{\text{ph2}}$ (19), $\delta(\text{CCH})_{\text{ph2}}$ (20)	1004	1056	1015	2	17	1056	1015	2	25
50	$\sigma(\text{CCN})_{\text{pyr}}$ (12)		1025	985	5	22	1024	984	2	48
51	$\beta(\text{CCC})_{\text{ph1}}$ (75)		1017	977	2	24	1017	977	57	94

TABLE VI cont.

Comparison of the experimental FT-IR wave numbers [cm^{-1}] for (2) compound and theoretical harmonic wave numbers [cm^{-1}] for hydrazone tautomer of (1) and (2) by B3LYP/6-31G(d,p) method.

ν	Assignments (%PED ^d)	Expt ^a	Theoretical							
			(1)				(2)			
			A ^b	B ^c	IR int.	R act.	A ^b	B ^c	IR Int.	R act.
52	$\beta(\text{CCC})_{\text{ph2}}$ (63)		1014	974	33	10	1016	977	4	26
53	$\gamma(\text{HNC})$ (75)		1005	966	8	195	1006	967	40	209
54	$\tau(\text{CCH})_{\text{ph2}}$ (72)		1001	962	0	1	1001	962	0	1
55	$\tau(\text{C-H})_{\text{ph1}}$ (85)	942	978	940	1	7	990	951	0	5
56	$\tau(\text{C-H})_{\text{ph2}}$ (93)		971	933	0	0	972	934	0	0
57	$\tau(\text{C-H})_{\text{ph1}}$ (90)		–	–	–	–	970	932	1	12
58	$\tau(\text{C-H})_{\text{ph2}}$ (86)		931	895	2	4	931	895	4	3
59	br(ph2-pyr) (27)		890	855	12	5	890	855	25	7
60	br(ph1) (20)	829	863	829	4	40	865	831	10	45
61	$\tau(\text{CCH})_{\text{ph2}}$ (94)		856	822	1	5	857	823	0	5
62	$\omega(\text{C-H})_{\text{ph1}}$ (58)		841	808	1	31	854	821	26	7
63	$\omega(\text{C-H})_{\text{ph1}}$ (83)		–	–	–	–	825	793	13	52
64	$\omega(\text{C-H})_{\text{ph2}}$ (35), $\gamma(\text{CCC})_{\text{pyr,ph2}}$ (31)	742	784	753	29	5	779	748	21	1
65	$\gamma(\text{OCC})_{\text{pyr}}$ (69), $\gamma(\text{CCC})_{\text{pyr}}$ (16)		765	735	32	6	765	735	27	7
65	$\gamma(\text{OCC})_{\text{pyr}}$ (62)		746	717	33	2	747	718	20	1
66	br(ph1) (33)		726	698	18	30	731	702	13	16
67	$\delta(\text{CCC})_{\text{pyr}}$ (36)		–	–	–	–	728	699	10	42
68	br(ph1) (34)	695	721	693	21	3	721	693	21	9
69	$\tau(\text{HNC})_{\text{pyr}}$ (41)		714	686	32	6	715	687	37	8
70	$\tau(\text{CCC})_{\text{pyr}}$ (65)		707	679	16	7	707	679	16	9
71	br(ph1-ph2-pyr) (33)		696	669	19	4	680	653	11	3
72	br(ph2) (15), $\nu(\text{CC})_{\text{pyr}}$ (10)	636	649	624	9	5	650	625	13	8
73	$\tau(\text{HNC})_{\text{pyr}}$ (18), $\sigma(\text{CCC})$ (10)		635	610	7	6	648	623	13	13
74	$\sigma(\text{CCC})_{\text{ph1}}$ (69)		625	601	1	15	641	616	1	30
75	$\tau(\text{HNC})_{\text{pyr}}$ (10), $\sigma(\text{CCC})_{\text{ph2}}$ (20)		624	600	2	3	623	599	2	3
76	$\nu(\text{C-Br})$ (12)		–	–	–	–	562	540	26	78
77	$\gamma(\text{CCC})_{\text{pyr}}$ (17), $\tau(\text{NCC})_{\text{pyr}}$ (41)	555	541	520	0	3	541	520	0	3
78	$\tau(\text{CCC})_{\text{ph1}}$ (19), $\tau(\text{CCN})_{\text{ph1}}$ (10)		530	509	32	17	528	507	11	36
79	$\tau(\text{CCC})_{\text{ph2,pyr}}$ (35)	508	520	500	3	2	520	500	0	8
80	$\sigma(\text{CCN})_{\text{ph1}}$ (10)		502	482	11	4	506	486	4	5
81	$\sigma(\text{CCN})_{\text{ph1}}$ (16), $\sigma(\text{OCN})_{\text{pyr}}$ (25)		469	451	2	16	474	455	4	34
82	$\sigma(\text{NCC})_{\text{pyr}}$ (34), $\sigma(\text{OCN})_{\text{pyr}}$ (10), $\nu(\text{CC})$ (13)		437	420	26	21	443	426	8	19
83	$\tau(\text{CCH})_{\text{ph1}}$ (10), $\tau(\text{CCC})_{\text{ph1}}$ (56), $\sigma(\text{CCN})_{\text{ph1}}$ (10)		417	401	2	21	424	407	1	30
84	$\tau(\text{CNN})_{\text{pyr}}$ (15), $\tau(\text{CCC})_{\text{ph2}}$ (11)		411	395	2	2	414	398	2	4
85	$\tau(\text{CNN})_{\text{pyr}}$ (11), $\tau(\text{CCC})_{\text{ph2}}$ (33)		402	386	5	14	406	390	1	8
86	$\sigma(\text{CCC})_{\text{pyr}}$ (17), $\sigma(\text{OCN})_{\text{pyr}}$ (26)		380	365	20	3	381	366	17	9
86	$\nu(\text{C-Br})$ (24)		–	–	–	–	347	333	27	7
87	$\gamma(\text{BrCC})$ (21), $\tau(\text{CCN})_{\text{ph1}}$ (39)		–	–	–	–	343	330	23	154
88	$\sigma(\text{BrCC})_{\text{ph1}}$ (19)		305	293	3	14	302	290	5	4
89	$\delta(\text{CCC})_{\text{ph1}}$, $\tau(\text{C-H})_{\text{ph2}}$, $\tau(\text{CCC})_{\text{pyr}}$		296	284	2	44	–	–	–	–
90	$\nu(\text{BrC})$ (10), $\tau(\text{CCC})_{\text{ph2}}$ (10)		289	278	3	44	288	278	6	7
91	$\gamma(\text{CCC})_{\text{pyr}}$ (16), $\tau(\text{NCC})_{\text{pyr}}$ (24)		264	254	1	3	266	256	1	2
92	$\gamma(\text{CNC})_{\text{pyr}}$ (16), $\sigma(\text{CCC})_{\text{ph1}}$ (10)		241	232	1	0	257	247	2	12
93	$\sigma(\text{BrCC})_{\text{ph1}}$ (14), $\gamma(\text{CNC})_{\text{pyr}}$ (16)		218	209	3	9	245	235	0	18
94	$\sigma(\text{BrCC})_{\text{ph1}}$ (23)		184	177	1	5	194	186	2	1
95	$\tau(\text{CNC})_{\text{pyr}}$ (50)		169	162	2	1	173	167	1	12
96	$\sigma(\text{CCC})_{\text{pyr}}$ (13), $\sigma(\text{NCC})_{\text{pyr}}$ (11)		–	–	–	–	161	155	1	3
97	$\sigma(\text{NCC})_{\text{pyr}}$ (12), $\sigma(\text{CCC})_{\text{pyr}}$ (12), $\tau(\text{CNN})_{\text{pyr}}$ (12)		139	134	3	16	154	148	3	10

ν stretching vibrations; β in-plane bending vibrations; γ out-of-plane bending vibrations; ω wagging; τ twisting; σ scissoring; δ rocking; br ring breath; s symmetric; as antisymmetric; pyr pyridone ring; ph benzene ring (the same below). ^a Data are taken from Ref. [11], ^b Unscaled wave number, ^c Scaled by a factor of 0.9608, ^d PED less than 10% are not shown.

hyperpolarizabilities (in a.u. and esu) using B3LYP/6-31G(d,p) method. This study reveals that (1) and (2) compounds have large first-order hyperpolarizabilities and have the potential applications in the development of NLO materials. The FT-IR spectra of hydrazone forms of (1) and (2) molecules have been satisfactorily interpreted in terms of hydrogen bonded hydrazone tautomer.

References

- [1] H. Çetişli, M. Karakuş, E. Erdem, H. Deligöz, *J. Incl. Phenom. Macro.* **42**, 187 (2002).
- [2] C.S. Wang, H.S. Fei, Y. Qiu, Y.Q. Yang, Z.Q. Wei, Y.Q. Tian, Y.M. Chen, Y.Y. Zhao, *Appl. Phys. Lett.* **74**, 19 (1999).
- [3] H. Zollinger, *Colour Chemistry*, VCH, Weinheim 1987.
- [4] C.C. Chen, I.J. Wang, *Dyes Pigm.* **15**, 69 (1991).
- [5] W. Huang, H. Qian, *Dyes Pigm.* **77**, 446 (2008).
- [6] W. Huang, *Dyes Pigm.* **79**, 69 (2008).
- [7] C. Lubai, C. Xing, G. Kunyu, H. Jiezheng, J. Griffiths, *Dyes Pigm.* **7**, 373 (1986).
- [8] A. Cee, B. Horáková, A. Lyčka, *Dyes Pigm.* **9**, 357 (1988).
- [9] G.S. Ušćumlić, D.Z. Mijin, N.V. Valentić, V.V. Vajs, B.M. Sušić, *Chem. Phys. Lett.* **397**, 148 (2004).
- [10] *Industrial Dyes: Chemistry, Properties, Applications*, Ed. K. Hunger, Wiley-VCH, 2003.
- [11] A. Alimmari, D. Mijin, R. Vukićević, B. Božić, N. Valentić, V. Vitnik, Ž. Vitnik, G. Ušćumlić, *Chem. Cent. J.* **6**, 71 (2012).
- [12] M.J. Frisch, G.W. Trucks, H.B. Schlegel, G.E. Scuseria, M.A. Robb, J.R. Cheesman, V.G. Zakrzewski, J.A. Jr. Montgomery, R.E. Stratmann, J.C. Burant, S. Dapprich, J.M. Millam, A.D. Daniels, K.N. Kudin, M.C. Strain, O. Farkas, J. Tomasi, V. Barone, M. Cossi, R. Cammi, J. Mennucci, G.A. Petersson, P.Y. Ayala, Q. Cui, K. Morokuma, N. Rega, P. Salvador, J.J. Dannenberg, D.K. Malich, A.D. Rabuck, K. Raghavachari, J.B. Foresman, J. Cioslowski, J.V. Ortiz, A.G. Baboul, B.B. Stetanov, G. Liu, A. Liashenko, P. Piskorz, J. Komaromi, R. Gomperts, R.L. Martin, D.J. Fox, T. Keith, M.A. Al-Laham, C.Y. Peng, A. Nanayakkara, M. Challacombe, P.M.W. Gill, B. Johnson, W. Chen, M.W. Wong, J.L. Andres, C. Gonzalez, M. Head-Gordon, E.S. Replogle, J.A. Pople, *Gaussian 09*, Revision A.1, Gaussian Inc., Wallingford (CT) 2009.
- [13] M.J. Frisch, G.W. Trucks, H.B. Schlegel, *GaussView*, Ver. 5.0.9, Semichem. Inc., Shawnee Mission (KS) 2009.
- [14] A.D. Becke, *J. Chem. Phys.* **98**, 5648 (1993).
- [15] C. Lee, W. Yang, R.G. Parr, *Phys. Rev. B* **37**, 785 (1988).
- [16] M.H. Jamroz, *VEDA 4 Program*, Warsaw 2004.
- [17] A.P. Scott, L. Radom, *J. Phys. Chem.* **100**, 16502 (1996).
- [18] J.B. Foresman, A. Frisch, *Exploring Chemistry with Electronic Structure Methods*, Gaussian Inc., Pittsburgh 1996.
- [19] E.D. Glendening, C.R. Landis, F. Weinhold, *Comput. Mol. Sci.* **2**, 1 (2011).
- [20] T.C. Koopmans, *Physica (Amsterdam)* **1**, 104 (1933).
- [21] P. Senet, *Chem. Phys. Lett.* **275**, 527 (1997).
- [22] L. Pauling, *The Nature of the Chemical Bond*, Cornell University Press, Ithaca 1960.
- [23] A. Hinchliffe, B. Nikolaidi, H.J.S. Machado, *Int. J. Mol. Sci.* **5**, 224 (2004).
- [24] A.D. Buckingham, *Adv. Chem. Phys.* **12**, 107 (1967).
- [25] A.D. Mclean, M. Yoshimine, *J. Chem. Phys.* **47**, 1927 (1967).
- [26] C. Lin, K. Wu, *Chem. Phys. Lett.* **321**, 83 (2000).
- [27] J.P. Abraham, D. Sajjan, I.J. Hubert, V.S. Jayakumar, *Spectrochim. Acta A* **71**, 355 (2008).
- [28] P. Karamanis, C. Pouchan, G. Maroulis, *Phys. Rev. A* **77**, 013201 (2008).
- [29] A. Ben Ahmed, H. Feki, Y. Abid, H. Boughzala, A. Mlayah, *J. Mol. Struct.* **888**, 180 (2008).
- [30] A. Streitwieser Jr., *Molecular Orbital Theory for Organic Chemists*, Wiley, New York 1961.
- [31] K. Fukui, *Science* **218**, 747 (1982).
- [32] J. Dostanić, D. Mijin, G. Ušćumlić, D.M. Jovanović, M. Zlatar, D. Lončarević, *Spectrochim. Acta A* **123**, 37 (2014).
- [33] J. Mirković, J. Rogan, D. Poletti, V. Vitnik, Ž. Vitnik, G. Ušćumlić, D. Mijin, *Dyes Pigments* **104**, 160 (2014).
- [34] A. Esme, S.G. Sagdinc, *J. Mol. Struct.* **1048**, 185 (2013).
- [35] A. Temel, S. Ozbey, N. Ertan, *Dyes Pigm.* **32**, 237 (1996).
- [36] L.C. Abbott, S.N. Batchelor, J. Oakes, B.C. Gilbert, A.C. Whitwood, J.R.L. Smith, J.N. Moore, *J. Phys. Chem. A* **109**, 2894 (2005).
- [37] M.R. Almeida, R. Stephani, H.F. Dos Santos, L.F.C. De Oliveira, *J. Phys. Chem. A* **114**, 526 (2010).
- [38] V. Bertolasi, L. Nanni, P. Gilli, V. Ferreti, G. Gilli, *New J. Chem.* **18**, 251 (1994).
- [39] F.H. Allen, O. Kennard, D. Watson, L. Brammer, A.G. Orpen, R. Taylor, *J. Chem. Soc.* **2**, S1 (1987).
- [40] D.B. Pendergrass, I.C. Paul, D.Y. Curtin, *J. Am. Chem. Soc.* **94**, 8730 (1972).
- [41] P.K. Chattaraj, S. Nath, B. Maiti, *Computational Medicinal Chemistry for Drug Discovery*, Marcel Dekker, New York 2003.
- [42] R.G. Parr, W. Yang, *Density Functional Theory of Atoms and Molecules*, Oxford University Press, Oxford 1989.
- [43] P. Politzer, J. Murray, *Theor. Chem. Acc.* **108**, 134 (2002).
- [44] P. Politzer, J.S. Murray, *Theoretical Biochemistry and Molecular Biophysics: A Comprehensive Survey*, Adenine Press, New York 1991.
- [45] O. Prasad, L. Sinha, N. Kumar, *J. At. Mol. Sci.* **1**, 201 (2010).
- [46] Y.G. Sidir, I. Sidir, *J. Sci. Technol.* **1**, 7 (2011).

- [47] F. Weinhold, C.R. Landis, *Chem. Educ. Res. Pract. Eur.* **2**, 91 (2001).
- [48] M. Kaur, Y.S. Mary, H.T. Varghese, C.Y. Panicker, H.S. Yathirajan, M.S. Siddegowda, C. Van Alsenoy, *Spectrochim. Acta Part A Mol. Biomol. Spectrosc.* **98**, 91 (2012).
- [49] Y. Matsuda, T. Ebata, N. Mikami, *J. Chem. Phys.* **110**, 8397 (1999).
- [50] G. Varsanyi, *Assignment for Vibrational Spectra of Seven Hundred Benzene Derivatives*, Academic Kiado, Budapest 1973.
- [51] M. Jag, *Organic Spectroscopy-Principles and Applications*, Narosa Publ. House, New Delhi 2001.
- [52] M. Snehalatha, C. Ravikumar, I.J. Hubert, *Solid State Sci.* **11**, 1275 (2009).
- [53] J.B. Labbert, H.F. Shurvel, L. Verbit, R.G. Cooks, G.H. Stout, *Organic Structural Analysis*, Macmillan Publ. Co. Inc., New York 1976.
- [54] H.P. Gümüş, O. Tamer, D. Avci, Y. Atalay, *Spectrochim. Acta Part A Mol. Biomol. Spectrosc.* **132**, 183 (2014).
- [55] A.J. LaPlante, H.D. Stidham, *Spectrochim. Acta A* **74**, 808 (2009).
- [56] W. Zierkiewicz, D. Michalska, T.H. Zeegers-Huyskens, *J. Phys. Chem. A* **104**, 11685 (2000).